LBNL-58659

ERNEST ORLANDO LAWRENCE
BERKELEY NATIONAL LABORATORY

Per-Pixel Lighting Data Analysis

Mehlika Inanici, Ph.D.

Environmental Energy Technologies Division
Department of Building Technologies
Lighting Research Group
1 Cyclotron Rd., MS 46-0125
Berkeley CA 94720
Phone: (510) 486-4531
Fax: (510) 486-4089
MInanici@lbl.gov

August 2005

This work was supported by the Assistant Secretary for Energy Efficiency and Renewable Energy, Office of Building Technology, Building Technologies Program, of the U.S. Department of Energy under Contract No. DE-AC02-05CH11231.

Per-Pixel Lighting Data Analysis

Abstract

This report presents a framework for per-pixel analysis of the qualitative and quantitative aspects of luminous environments. Recognizing the need for better lighting analysis capabilities and appreciating the new measurement abilities developed within the LBNL Lighting Measurement and Simulation Toolbox, "Per-pixel Lighting Data Analysis" project demonstrates several techniques for analyzing luminance distribution patterns, luminance ratios, adaptation luminance and glare assessment. The techniques are the syntheses of the current practices in lighting design and the unique practices that can be done with per-pixel data availability. Demonstrated analysis techniques are applicable to both computer-generated and digitally captured images (physically-based renderings and High Dynamic Range photographs).

Table of Contents

1. INTRODUCTION

Emerging and existing technologies for lamp, ballast, and control systems facilitate frequent switching and dimming applications, automated response for daylight harvesting, and individual addressability [1]. Hence, current lighting design trends promote dynamic lighting conditions with automated and manual controls of the intensity, location, distribution and color of lighting systems. Measurement and analysis of such environments comes with challenges.

With the successful development of the **Lighting Measurement and Simulation Toolbox** in FY2004, significant progress has been made towards the achievement of better lighting measurement tools [2]. HDR photography technique provides a camera independent, low cost, and accessible solution for an advanced data acquisition system that can capture luminance values in:

- High resolution, that allows to study the temporal and spatial variability within the environment;
- High Dynamic Range (HDR); that covers the total human visual range from starlight to sunlight (10^{-8} to 10^{6} cd/m^2); and
- Large field of view, that covers the total human vision, which is 180° horizontally and 130° vertically.

Recognizing the need for better lighting analysis capabilities and appreciating the new measurement abilities developed within the toolbox, the key objective of FY2005 is to demonstrate several per-pixel data analysis techniques. The milestone of the project involves the development and limited demonstration of relevant lighting techniques and metrics for determining luminance distribution patterns, luminance ratios, adaptation luminance and glare assessment. Per-pixel data analysis techniques support the lighting design and application strategies through informed decision making processes. The end result is an enabling technology that can facilitate significant energy savings, occupant satisfaction and productivity improvements. This report is the deliverable for the FY2005 activities of the Lighting Measurement, Simulation, and Analysis Toolbox.

2. PER-PIXEL DATA ANALYSIS

Per-pixel lighting data is invaluable for the qualitative and quantitative analysis of luminous environments.

Per-pixel data acquisition, generation, and analysis are the keystones in the Lighting Measurement, Simulation, and Analysis Toolbox. Per-pixel luminance data can be obtained through either physically-based rendering tools[1] or HDR photography techniques [4, 5] (Fig. 1).

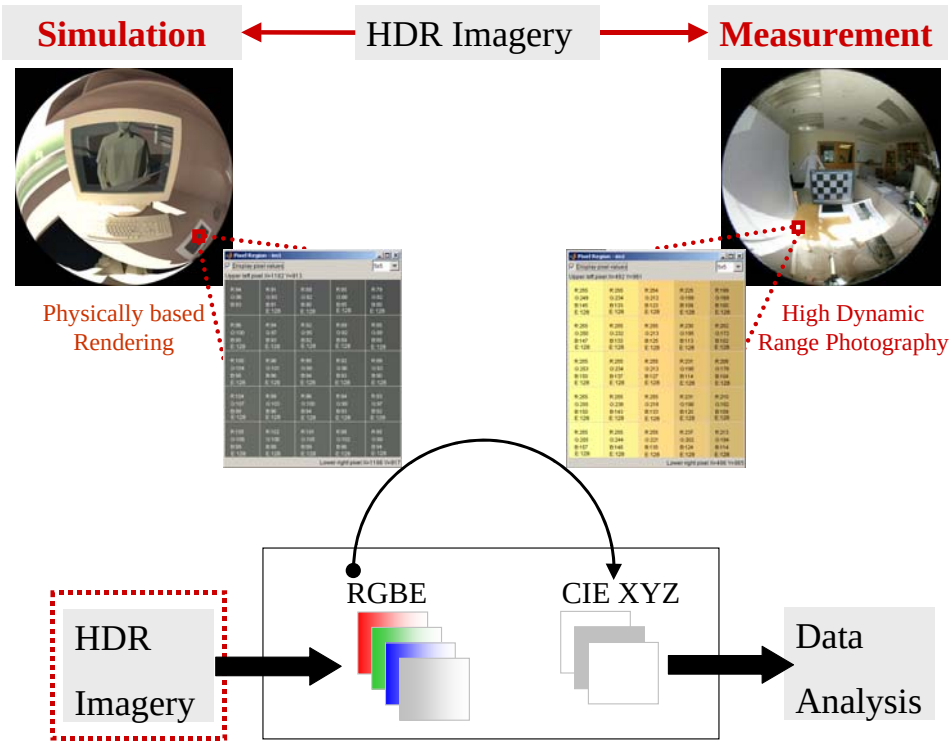

Fig. 1 Per-pixel data extraction from physically based renderings and HDR photography

Per-pixel data analysis techniques developed in the **Virtual Lighting Laboratory** © (VLL) [6] form the basis of the analysis options in the toolbox. The VLL is a computational methodology and a computational tool, where lighting quantities are

[1] Tools such as Radiance Lighting Simulation and Rendering System [3] or any other lighting simulation software that can provide High Dynamic Range (HDR) imagery can be used for per-pixel analysis.

extracted from Radiance images and analyzed through mathematical operations and computational routines on a pixel scale. The techniques shown in this report can operate with any HDR image; both computer-generated or digitally captured. The image format is RGBE [7] (a.k.a. *.hdr or *.pic). Floating point RGB value of each pixel is transformed into CIE Trisimulus Color Space (CIE XYZ) based on the Standard CIE Colorometric Functions (Detailed explanation is available in FY2004 Deliverable and LBNL-Report#57545 [2]).

Per-pixel lighting data is invaluable in evaluating the qualitative and quantitative aspects of a luminous environment. Utilization of several metrics to determine visual comfort and performance are exemplified through sets of images captured at the New York Times (NYTimes) Headquarters Mockup Building. The mockup is a 4500 sq.ft. building that constitutes a portion of one floor of the NYTimes Headquarters building that is being built in the Times Square in NYC. The mockup is constructed in Queens (NYC) on the parking lot of the NYTimes printing facility to test the hardware and control solutions. An image database consisting of 150 High Dynamic Range (HDR) photographs has been assembled from multiple exposure sequences that were captured in November 2004. With controlled shading and lighting systems, the mock-up provided a unique opportunity to evaluate different lighting situations. Therefore, the database is consistent of a wide range of lighting conditions of open and private office spaces, operated with manual and automated shade fabric and lighting control systems.

2.1 AVAILABLE AUTOMATED TOOLS:

The per-pixel lighting data can be processed to perform lighting analyses with detail, flexibility and rigor that may be infeasible or impossible with traditional lighting analysis approaches. One obvious application of per-pixel data is to process it with automated analysis tools in currently available lighting software. Examples include the ‘luminance false color images’, ‘luminance iso contour lines’ (2.1.1), and ‘glare analysis’ modules (2.1.2) presented in this report.

2.1.1. False Color Images and Iso-Contour Lines:

False color images and iso-contour lines are utilized to demonstrate HDR lighting data, which cannot be displayed in absolute values and full range through conventional display devices (LCD and CRT screens) or printed media. In false color images (falsecolor [8]), a range of colors is assigned to a range of luminance (or illuminance) values. Such analysis is useful to understand the dynamic range and to visualize the spatial luminance (or illuminance) distributions within a space.

Fig. 2 is an example of false color analysis of the shade fabric operation. The shade fabric has been operated in one of the 4 modes (a. open, b. drawn to cover the top portion of the window, c. drawn to cover the middle portion of the window, and d. fully drawn). The impact of the different operating modes of the shade fabric has been captured with HDR photographs. In false color images, blue tones represent the low luminance values (<200 cd/m^2, a.k.a. Nits), and red tones represent the high luminance values (> 2000 cd/m^2) in the scene. The position of the shade fabric not only determines the window luminance, but also the luminance distribution within the whole field of view. An adequate amount of variation in luminance assures visual comfort, visibility, and aesthetically pleasing environment. The quantities that deviate significantly from the average or target values may indicate poor lighting conditions [20].

Iso-contour line analysis is composed of colored contour lines that are superimposed on the original image to demonstrate the distribution of the luminance values (Fig. 3). A single image not only illustrates the original true color image but also full distribution of luminances with contour lines drawn in equal steps.

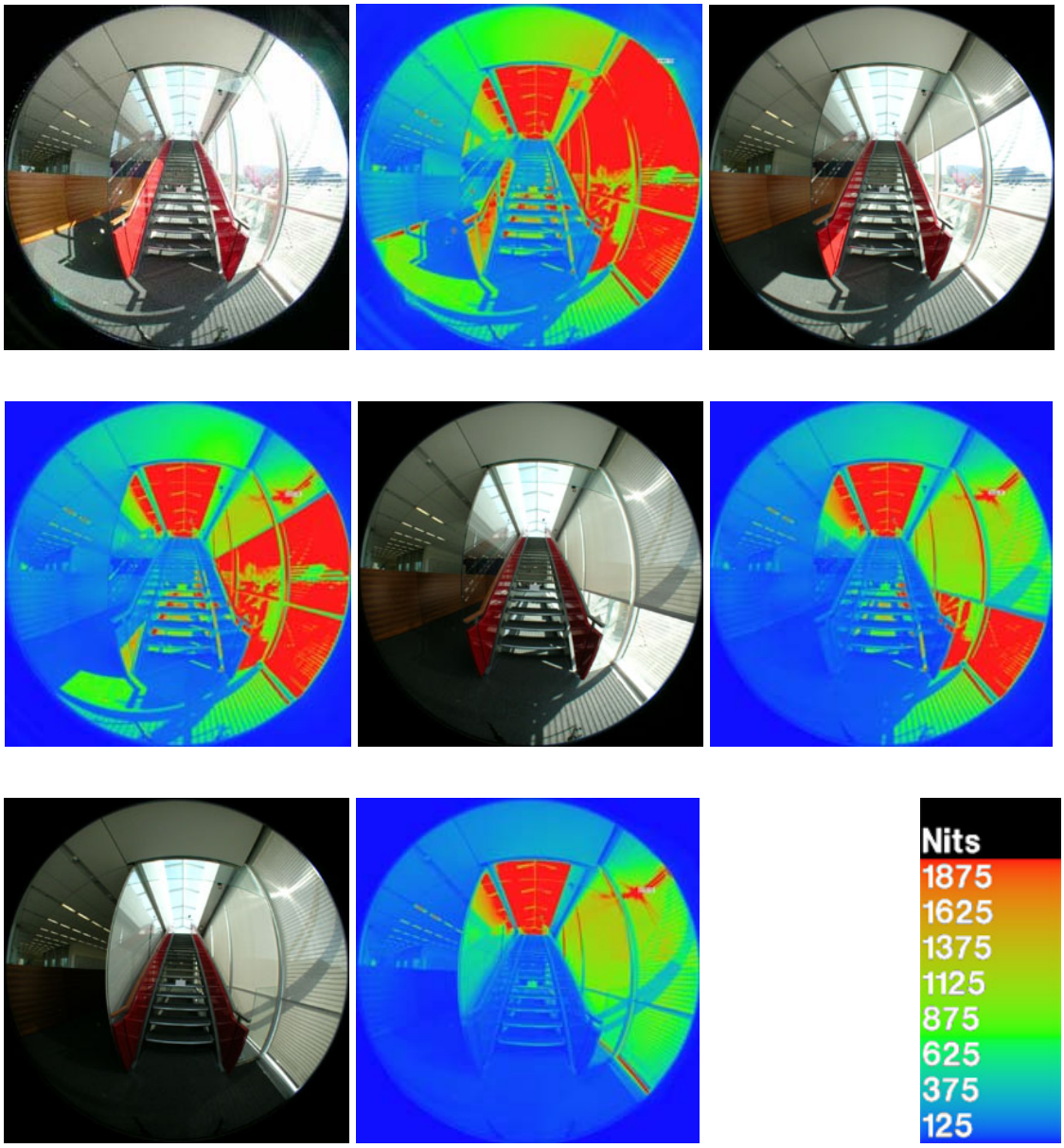

Fig. 2 False color images generated from HDR photographs that capture the staircase area on the south part of the mockup as the shade fabric has been operated in one of the 4 modes. (The images are taken on 10/26/2004 between 12:52:46 – 12:59:59; aperture size of f/4; shutter speed between 1/15 - 1/4000 sec; clear sky)[2]

[2] All images in this report are captured with Nikon 5400 and FC-E9 Nikon fisheye lens. HDR images generated using Photosphere [9], post-processed with a digital vignetting filter as described in [2])

Fig. 3 Iso-contour analysis generated from a HDR photograph capturing the staircase area on the south part of the mockup. (Multiple exposure images are taken on 10/25/2004 between 16:04:36 – 16:05:23; aperture size of f/4; shutter speed between 1/4 - 1/500 sec; partly cloudy sky)

2.1.2 Glare Analysis

Automated glare analysis can be performed utilizing:

- Glare Module [10] (findglare [11], glarendx [12], xglaresrc [13]), or
- EvalGlare [14]

Glare Module [10] is an interactive script for locating glare sources and computing glare indices. Glare sources are identified based on a threshold value, which can be 1) specified by the user manually as a fixed luminance value or 2) computationally determined from the average luminance in the field of view. The adaptation level is computed using the indirect vertical illuminance as the background level. The following glare indices and quantities can be calculated [15]:

- Guth Visual Comfort Probability (VCP)
- CIE Glare Index (CGI)
- Unified Glare Index (UGI)
- BRS Glare Index
- Daylight Glare Index (DGI)
- Guth Disability Glare Rating
- Direct Vertical Illuminance
- Total Vertical Illuminance
- Indirect Vertical Illuminance

These glare indices form a collection of the major visual comfort metrics that are used in different countries around the world. VCP and DGI are the metrics that are currently being used in North America to evaluate discomfort glare.

Figure 4 illustrates a series glare analysis performed at a workstation on the Southwest part of the mockup. 4 photographs are taken in 4 cardinal orientations (East, South, West, and North). Note that glare calculations require fisheye images (180° degrees vertically and horizontally). Glare is a direction-specific metric, so 4 orientations represent 4 directions that the user is looking at. Glare indices are calculated at single viewpoints in these 4 orientations. Glare indices can also be calculated in multiple directions (for instance, to analyze glare due to head orientation). 360° angular images would be best to perform such calculations.

Fig. 4 demonstrates the glare sources as identified by the findglare program. The numeric information about the location, size, and luminance of the identified glare sources for Fig.4d are provided as an example in Table 1.

Table 1 Location, size, and luminance of identified glare sources from image 4.d.

Glare source	Direction dx, dy, dz)			Size (sr)	Luminance (cd/m2)
1	-0.68	0.57	-0.45	0.015	10877
2	-0.42	0.90	-0.09	0.026	12837
3	-0.16	0.96	-0.23	0.022	11911
4	-0.25	0.97	-0.07	0.018	10219
5	-0.77	0.64	-0.06	0.016	12738

The indirect illuminance for East, South, West, and North viewpoints are calculated as 529, 2204, 4367, and 2117 lx, respectively. The resultant DGI values are 11.0, 30.2, 21.4, and 22.3. As it can be seen from Fig. 5 and Table 2 (Multiple criterion scale of glare discomfort evaluation), glare is imperceptible in East direction, which is the actual task. It is acceptable in West and North directions, and intolerable in South direction (i.e. looking towards the sun).

Hopkinson-Cornell large-source glare studies have been conducted under controlled laboratory conditions with a largely illuminated diffusing screen (light from closely packed fluorescent lamps was diffused by an opal plastic screen) which had provided a uniform luminance source. Source size was varied from 10^{-3} sr. to the whole field of view, and the source luminance was varied between 3.5 and 15,500 cd/m^2 [17, 18]. Chauvel et.al [16] have studied the differences between the glare experienced from a real window and the glare calculated with the Hopkinson-Cornell index. The comparison showed that glare in real world environments is more tolerable than the glare index predicts. The difference is attributed to the psychological differences in the visual content of the field of view. Chauvel et.al. have modified the original Hopkinson-Cornell formula to take account of this effect. No direct sun was present in this study. Later, Boubekri et.al. [19] have studied the effect of window size and sunlight presence on glare. The results of their study indicate that the perceived glare with sunlight present in the environment is again lower than the DGI calculations. The difference is again attributed to the cheerful and positive effects of sunlight.

DGI is calculated in the Glare Module using 'Chauvel et.al' [16] formula (Equation 1).

$$DGI = 10 \log 0.478 \sum_{i=1}^{n} \frac{L_s^{1.6} \cdot \Omega^{0.8}}{L_b + 0.07 \cdot \omega^{0.5} \cdot L_s} \qquad \textit{(Equation 1)}$$

- L_s *Source luminance (cd/m^2)*
- L_b *Background luminance (cd/m^2)*
- Ω *Solid angular subtense of source modified for the effect of the position of its elements in different parts of the field of view*
- ω *Solid angular subtense of source at the eye of the observer (sr)*

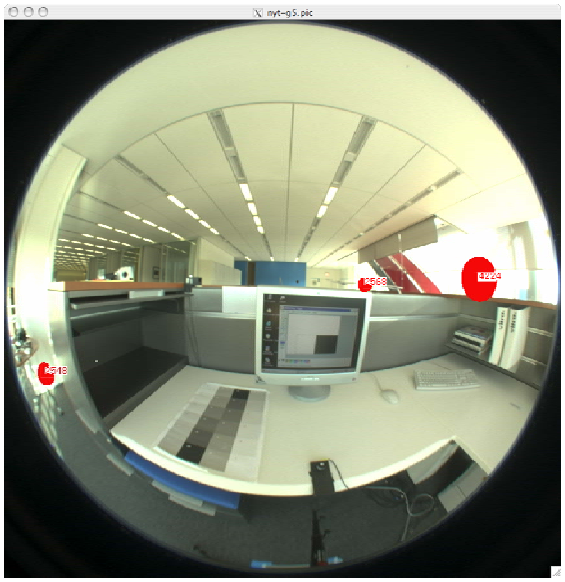

Observer is looking at East direction

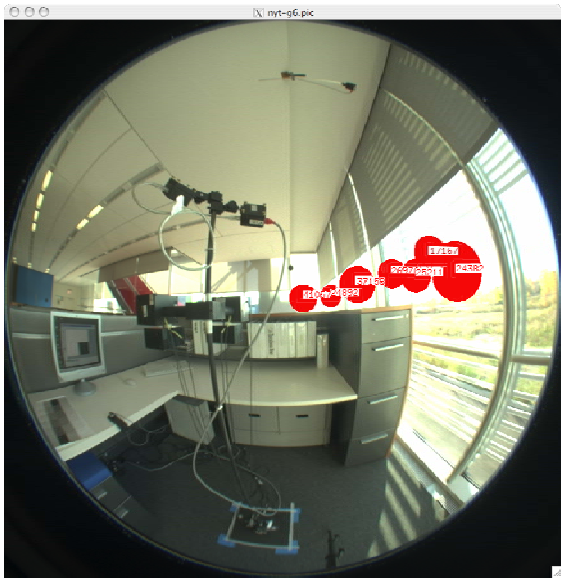

South

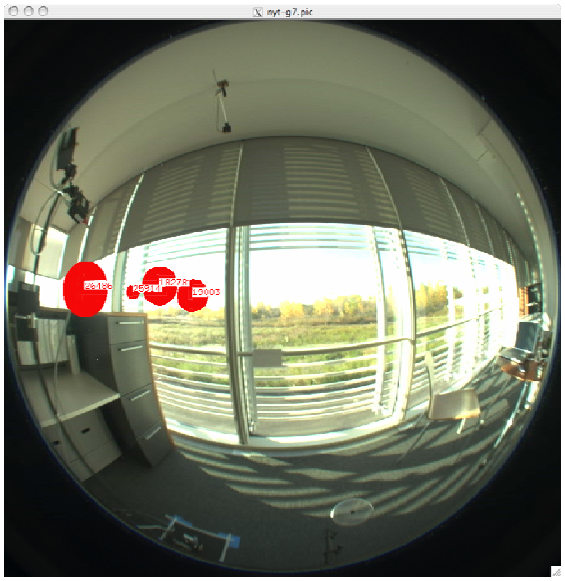

Observer is looking at West direction

North

Fig. 4 Glare analysis of an HDR photographs from a workstation on the South-West part of the mockup looking at 4 cardinal orientations: a) East b) South c) West d) North. The red circles are the identified glare sources. (Multiple exposure images are taken on 10/25/2004 between a) 16:02:44 - 16:03:40 b) 16:05:32 - 16:06:33 c) 16:07:11 – 16:08:05 d) 16:09:23 - 16:10:10; aperture size of f/4; shutter speed between 1/4 - 1/4000 sec; clear sky)

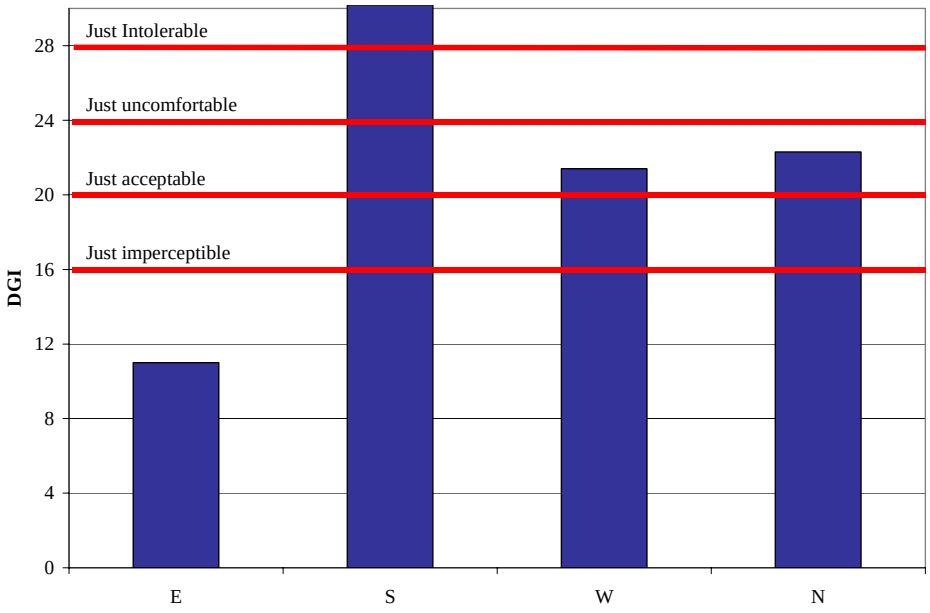

Fig. 5 Calculated DGI indices for images shown in Fig. 4.

Table 2 Multiple criterion scale of glare discomfort evaluation

Glare criterion corresponding to mean relation	DGI [16]
Just imperceptible	16
Noticeable	18
Just acceptable	20
Acceptable	22
Just uncomfortable	24
Uncomfortable	26
Just intolerable	28
Intolerable	30

Figure 6 illustrates a glare analysis performed at a workstation on the Northwest part of the mockup, looking towards East. The identified glare sources are from fluorescent lighting, so VCP is calculated as the glare index. The glare module identified nine glare sources for this location and view direction, and the resultant VCP is found as 98, which is the probability of the observers that will not experience discomfort (i.e. glare) when viewing this particular scene at this particular time.

Fig. 6 Glare analysis of a HDR photograph from a workstation on the Northwest part of the mockup. (Multiple exposure images are taken on 10/27/2004 between 13:28:53 – 13:29:50; aperture size of f/4; shutter speed between 1 - 1/1000 sec)

Guth Visual Comfort Probability (VCP) is "the probability that a normal observer does not experience discomfort when viewing a lighting system under defined conditions" [20]. VCP is the method currently adapted by the Illuminating Engineering Society of North America (IESNA) for evaluating direct glare in a room. The criterion is the luminance just necessary to cause discomfort [21]. The formulation provides ratings of visual comfort in terms of the percentage of people who will consider a given lighting system to be acceptable. Therefore, VCP value increases as discomfort decreases. VCP is calculated as follows [20]:

$$\text{Visual Comfort Probability } VCP = \frac{100}{\sqrt{2\pi}} \int_{-\infty}^{6.374-1.3227 \ln DGR} e^{-t^2/2} dt \qquad \textit{(Equation 2)}$$

$$\text{Discomfort Glare Rating } DGR = \left(\sum_{i=1}^{n} M_i \right)^{n^{-0.0914}}$$

$$\text{Index of Sensation } M = \frac{0.50 L_s Q}{PF_v^{0.44}}$$

$$\text{Luminance of Source } L_s$$

$$\text{Solid Angle Factor } Q = 20.4 w_s + 1.52 w_s^{0.2} - 0.075 .$$

$$\text{Position index } P = \exp\left[\begin{matrix} (35.2 - 0.31889\alpha - 1.22 e^{-2\alpha/9}) 10^{-3} \beta + \\ (21 + 0.26667\alpha - 0.002963\alpha^2) 10^{-5} \beta^2 \end{matrix} \right]$$

$$\text{Average Luminance for the Field of View}$$

$$F_v = \frac{L_w w_w + L_f w_f + L_c w_c + \sum L_s w_s}{5}$$

The principal research used to establish the VCP system involved luminances of magnitude comparable to those produced by fluorescent lamps. Further, experiments in simulated rooms have been used to confirm the extension from the laboratory to actual lighting installations. However, it is important to note that the testing and validation studies were done using lensed direct fluorescent systems only. Therefore, extrapolation to lamps and luminaires with significantly different luminance patterns has not been validated. It is not advised to apply VCP to very small sources such as incandescent and high-intensity discharge luminaires, to very large sources such as ceiling and indirect systems, or to non-uniform sources such as parabolic reflectors [20].

Automated glare calculations offer easy to use analysis tools for designers and researchers. Traditionally, one obstacle for utilize the glare metrics has been the difficulty of measuring the parameters required for the calculation. HDR photography technique provides a solution for this barrier. However, it is important to note that these glare indices were developed long ago, when the researchers did not have measuring capabilities that are available today. The glare studies were predominantly based on oversimplifications and unpractical assumptions. Therefore, utilization of these indices with HDR images inherits these oversimplifications. Moreover, DGI and VCP were developed to determine glare from large area sources and fluorescent lamps, respectively; and neither of them is capable of determining glare from integrated daylighting and electric lighting solutions. There is a need for new glare indices that are developed by utilizing the advanced (per-pixel) measuring capabilities.

EvalGlare [14] is a new tool for evaluating daylight glare. It is being developed as a European research project in Freiburg (Germany) and Copenhagen (Denmark). Evalglare can also be used to calculate glare from HDR photographs. Glare sources also identified based on a threshold value, which can be 1) specified by the user manually as a fixed luminance value, 2) computationally determined based on average luminance in the field of view, or 3) computationally determined based on a user specified task location. Note that EvalGlare is still in an experimental status and is not validated yet.

2.2 NUMERICAL METHODS

The readily available automated tools are useful to the lighting professionals, but the real potential of the HDR imagery comes with flexible per-pixel data analysis techniques that

can be custom tailored for the specific needs of a project or research. A few of the applications are exemplified here:

2.2.1 Luminance Distribution, Ratios and Contrast:

> *The spatial distribution of light is a measure of luminance (and/or illuminance) variability across a plane or surface [22]. The simplest and most crude way is to look at the maximum, minimum, and average values in the whole scene, on a surface, or in a region of interest. In the physical world, spatial distribution of light is determined through multi-point measurements. The major drawback is that large numbers of measurements have to be done in a grid pattern. The number of points determines not only the resolution of the distribution pattern, but also the precision of average calculations. Locating the maxima and minima is not always a straightforward task. Due to the spatial variations, measuring one point versus another could produce different quantities and ratios, which could point to an ambiguous and non-repeatable measuring process [6].*

Per-pixel data is a very convenient way for studying the luminance values and distributions. The maximum, minimum, and average values are calculated from a matrix that can correspond to the whole scene (i.e., circular part of the fisheye); a surface (i.e., architectural elements such as wall, window, table, ceiling, etc); or a region of interest (such as a task area or part of a human visual field of view).

2.2.1.1 Evaluation by Region of Interest:

Masks can be utilized to isolate the elements or region of interest from the rest of the scene. Masking is done by filtering the original image by a binary image that has the same resolution. The binary image contains ‘1’s for pixels that are part of the region of interest and ‘0’s for the rest of the image. The filtered values are the quantities in the original image (essentially, the lighting matrix) that correspond to pixel coordinates with 1’s in the binary image. They are stored in a separate matrix, in which each element of the matrix corresponds to luminance value of a single pixel. Therefore, mathematical and statistical operations (such as minimum, maximum, average, standard deviation, frequency, and so on) can be applied to pixel values for inquiring various properties of the region of interest.

There are multiple ways of creating the binary masks. For instance, Matlab Image Processing Toolbox® [23] offers several useful functions. Polygon-based region of interest is specified by supplying the pixel coordinates or simply clicking on the vertices of a polygon in the image. It is effective when the region of interest has an uncomplicated geometry. Intensity-based region of interest is specified by supplying a range of intensities for pixel values. The third option is to employ edge detection functions to detect various object boundaries in an image. This function returns a binary image that contains 1's for edges and 0's in the rest of the image. Other image processing software, such as PhotoShop® [24], can also be used to create the masking images.

Figure 7 demonstrates south façade as the shade fabric is operated in different modes (a. shade open, b. drawn to cover the top portion of the window, c. drawn to cover the middle portion of the window, and d. fully drawn). The minimum, maximum, and average luminance values in the whole scene are given in Fig. 8.

Figure 9 demonstrates the selection and masking of a region of interest. The region of interest in this case is chosen as the mid-portion of the window. According to the New York Times Headquarters procurement specifications [25], this portion of the window should not exceed 2000 cd/m^2 when the orb of the sun is not within the immediate field of view. Pixels corresponding the mid-portion of the window are isolated from the rest of the scene by using the mask in Fig. 9.b. These pixels are compared between images 7.a and 7.c. The average luminance of the mid-portion of the window drops from 5,223 to 612 cd/m^2, as the shade fabric is drawn from open position to cover the mid-portion of the window. This kind of analysis is useful to compare quantities against standards, recommendations, or specifications.

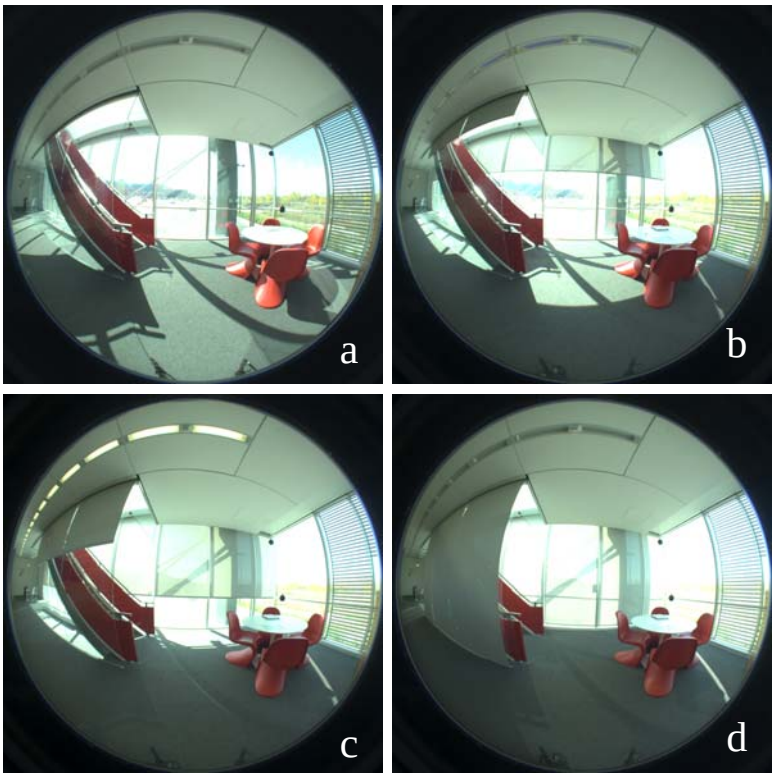

Fig. 7 Photographs that capture the south part of the mockup as the shade fabric has been operated in one of the 4 modes. (Multiple exposure images are taken on 10/26/2004 between a) 11:38:46 - 11:39:41 b) 11:40:42 - 16:41:43 c) 11:43:34 – 11:44:41 d) 11:46:58 - 11:47:54; aperture size of f/4; shutter speed between 1/4 - 1/4000 sec; partly cloudy sky)

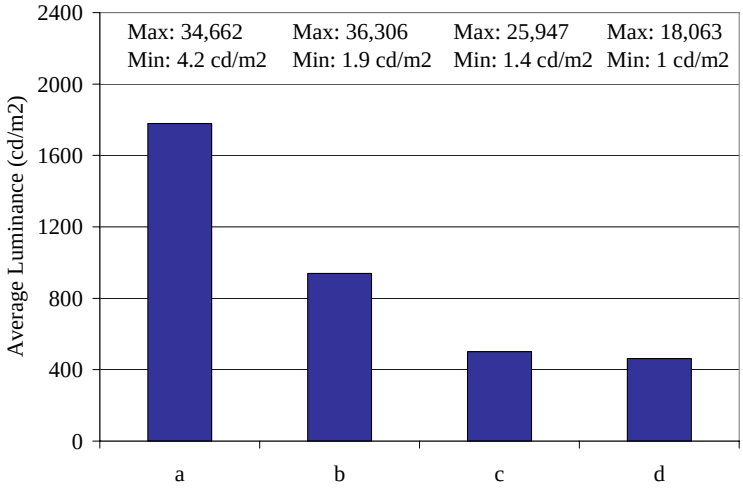

Fig. 8 Minimum, maximum, and average luminance values in the whole scene for the images shown in Fig. 7.

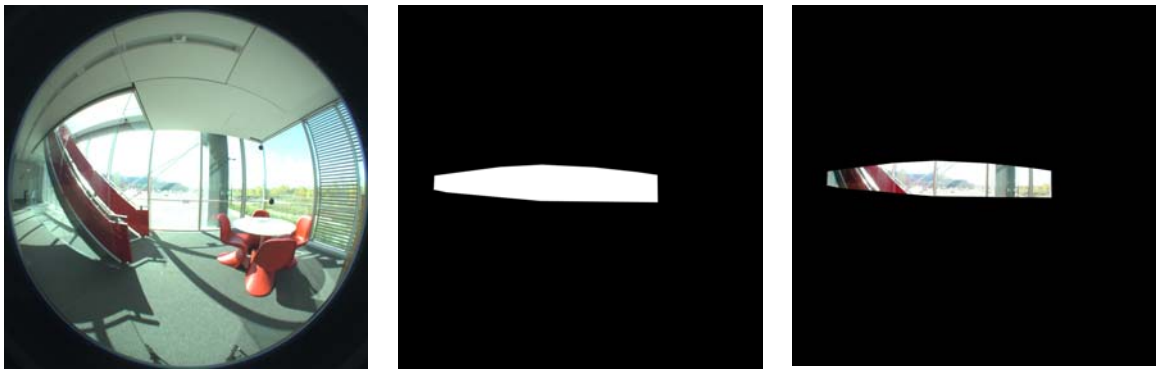

Fig. 9 Masking of the mid-portion of the window

Although the average mid-portion window luminance is within specifications, the maximum window luminance in this part is 17,099 cd/m^2, which is well above the specified 2,000cd/m^2 limit. More detailed analysis can be performed by employing histograms. Histograms in Fig. 10 are used to graphically summarize the distribution of pixel (luminance) values in the mid-portion of the window. The left and right columns correspond to shade positions in 7.a and 7.c. The range of the data is divided into equal-sized bins (luminance values as shown in the horizontal axis). Then for each bin, the number of pixels that fall into each bin are counted and reported as frequency in the vertical axis. The upper histograms show the luminance distributions for the whole range of data. The lower histograms show the data between 0 to 2,000 cd/m2.

Criterion rating quantifies the probability that a specific criterion is met within a defined area [20]. It can be expressed for various lighting quantities such as luminance, illuminance, contrast, and CCT. The criterion rating can be calculated best using per-pixel data as follows [6]:

$$\text{Pixel Criterion Rating}\,(\%) = \frac{\text{Number of pixels satisfying the criterion} * 100}{\text{Total number of pixels}} \quad \textit{(Equation 3)}$$

As it can be seen from the right histograms (shade position ‘c’), although the maximum luminance is quite high (17,099 cd/m^2), the majority (pixel criterion rating of 99%) of the pixels are below 2,000cd/m^2 level. The maximum luminance value occurs in few pixels, which are peak luminance values at small angular size that indicate “points of interest” or “sparkle” rather than glare sources; therefore they can be ignored. On the other hand, only 55% of the total pixels satisfy the 2,000cd/m2 specification in the shade position ‘a’,

pointing to large areas of high luminance values that can cause discomfort and visibility problems.

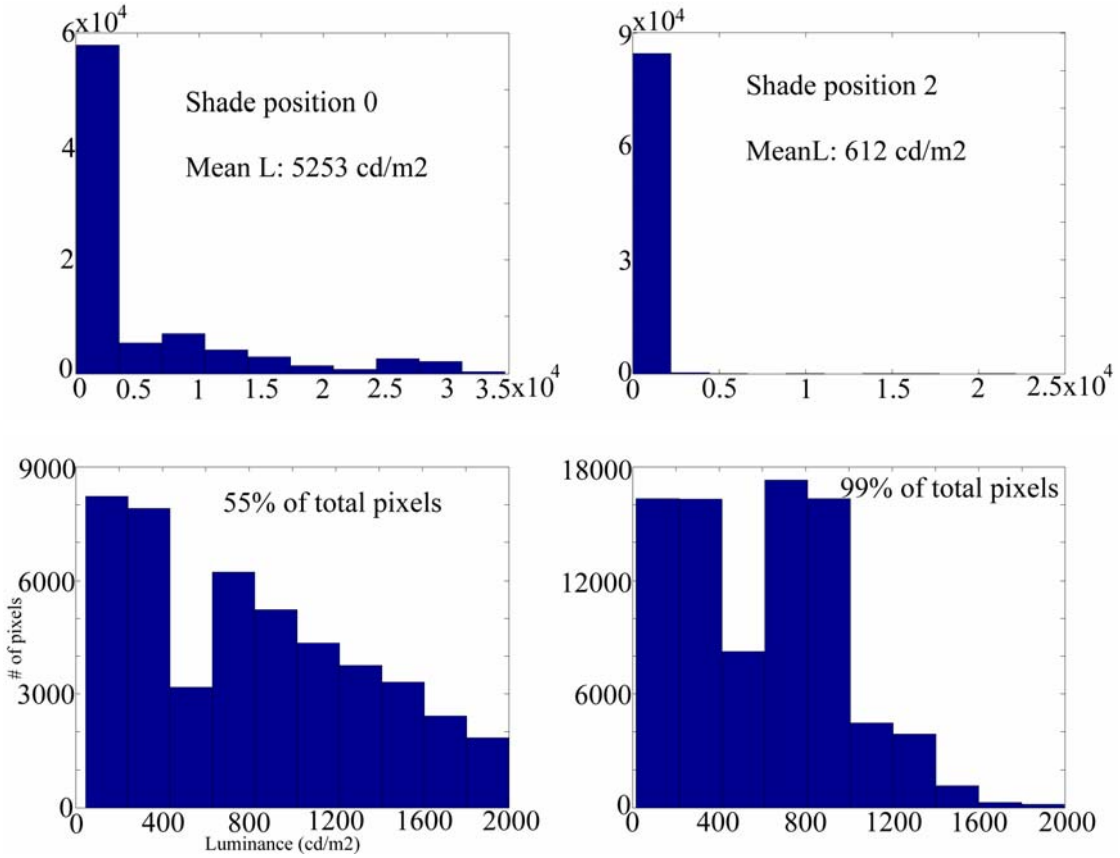

Fig. 10 Histograms of pixel (luminance) values in the mid-portion of the window for shade positions ‘a’ and ‘c’

2.2.1.1 Evaluation by Image Subtraction:

Another way to study the lighting distributions, especially to compare alternative lighting systems, is to apply image subtraction method. Fig.11 illustrates a workstation with shade fabric in position ‘a’ and ‘b’ (a. open, b. drawn to cover the top portion of the window). The third image illustrates the subtraction of image b from a. The luminance distributions of the alternative scenes are quite different. Fig. 11.d-f shows the areas where the luminance difference is more than 100 cd/m^2 (2 logarithmic units), 1,000 cd/m^2 (3 logarithmic units), and 10,000 cd/m^2 (4 logarithmic units), respectively. These are differences that are perceivable by the human eye. Fig. 11.d-f

demonstrates that the shade fabric position 'b' is effective in controlling the window luminance[3], but it has impact on all other architectural surfaces (such as desk surface and ceiling)[4].

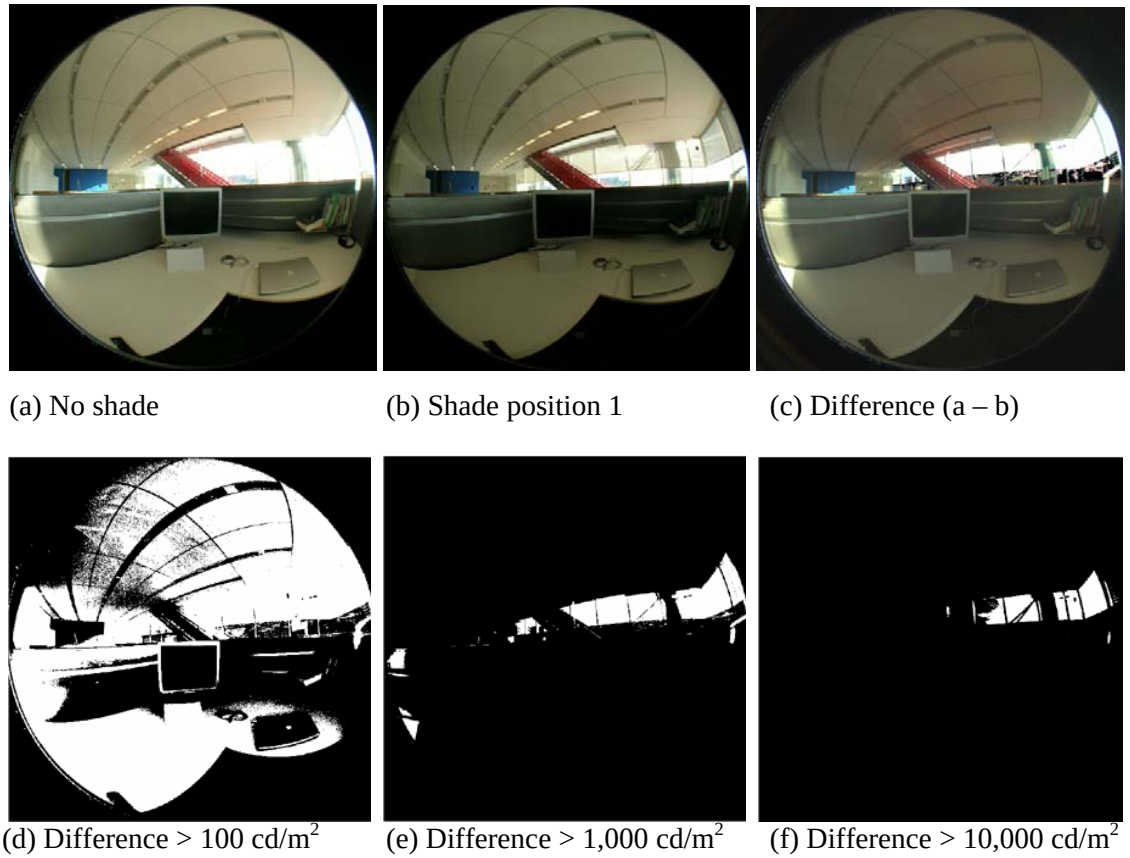

(a) No shade (b) Shade position 1 (c) Difference (a – b)

(d) Difference > 100 cd/m^2 (e) Difference > 1,000 cd/m^2 (f) Difference > 10,000 cd/m^2

Fig. 11 Image subtraction method for comparing the luminance distributions between alternatives 11.d-f demonstrate the areas with 2,3,and 4 logarithmic units of luminance difference between images a and b. (Multiple exposure images are taken on 10/27/2004 between a) 16:12:25 - 16:13:24 b) 16:14:35 - 16:15:34; aperture size of f/4; shutter speed between 1/4 - 1/4000 sec; clear sky)

2.2.1.1 Evaluation by Luminance Ratios:

In lighting practice, it is common to compare luminance ratios on task and certain architectural elements such as wall, ceiling, and surround. Luminance variation across the immediate task has to be kept within 3:1 range, where the task luminance is suggested to be higher than the immediate surrounding. Ceiling and walls are recommended to be within a 3:1 luminance ratio. Distant room surfaces are preferred to be within 10:1 luminance range (40:1 maximum). In offices with computer tasks, the maximum allowable ceiling luminance is 850 cd/m^2, whereas the desirable ceiling luminance is to

[3] The window luminance is decreased by 1,000 cd/m^2 or more (>10,000 cd/m^2), as observed in Fig. 11e-f.
[4] The surface luminance values on the desk and ceiling are also decreased by 100 cd/m^2 or more.

be less than 425 cd/m^2 (this is a recommendation for CRT screen and does not apply for LCD screens). Maximum to the minimum ceiling luminance ratios up to 8:1 are acceptable whereas 2:1 ratios are desirable. These recommendations are specified to avoid extreme luminance differences since the human vision cannot adapt to wide range of luminances at once. They are the generalized results of studies that investigate the effects of different lighting variables on visual comfort and performance [20, 22].

The scene in Fig. 12 is a workstation in open plan office space. The scene is decomposed into elements, which are the computer screen, paper, wall behind the task, table, and the window. It is a trivial task to calculate the average and locate the minima and maxima in each element. Luminance range and ratios for each element and among the elements are identified and compared with IESNA recommendations. For this particular viewpoint and time, the measured luminance ratios are found out to be within recommendations.

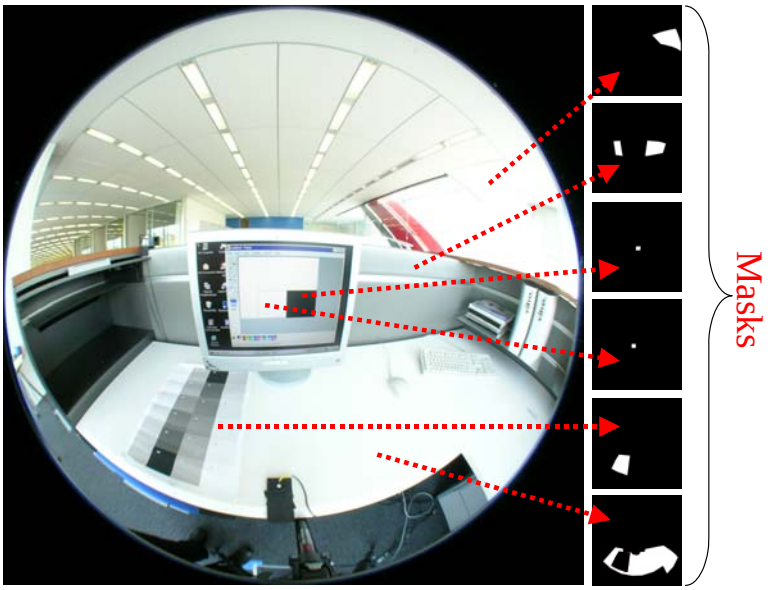

Window	Min L	9 cd/m2
	Max L	19522
	Mean L	669
Wall	Min L	7 cd/m2
	Max L	1297
	Mean	233
Screen	White	230cd/m2
	Black	15
	Contrast	0.93
Paper	White	239cd/m2
	Black	14
	Contrast	0.94
Table	Min L	1 cd/m2
	Max L	2051
	Mean L	131

	E (lux)	Max. L (cd/m2)	L ratio (task: surround)	L ratio (task: wall)
IESNA	200-300	850	3:1	10:1, 40:1 max

Fig. 12 Decomposition of the scene into architectural elements to study the luminance ratios (Multiple exposure images are taken on 10/25/2004 between 10:11:02 – 10:12:09; aperture size of f/4; shutter speed between 1 - 1/2000 sec; partly cloudy sky)

A more detailed analysis of luminance distribution can be performed utilizing histograms. Fig. 13 illustrates luminance distributions when the observer is looking at the computer task. The first histogram demonstrates that the data is unimodal and skewed to the left. Although the data spreads between approximately 0 to 30,000 cd/m^2, 98% of the pixels fall in the luminance bin that is between 0 to 1,000 cd/m^2. These graphs suggest that the luminance distribution pattern is in close range throughout the scene with adequate amount of variation; and except for the few outliers, quantities do not deviate significantly from the rest of the pixels.

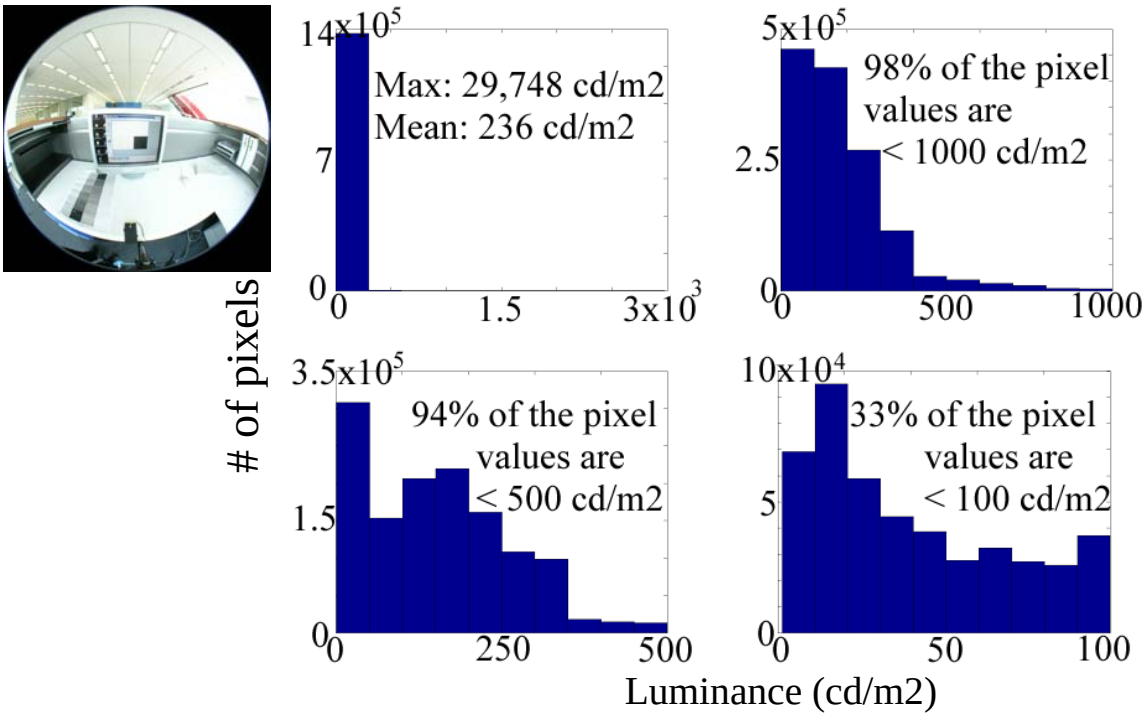

Fig. 13 Histograms of pixel (luminance) values in the scene as the observer is looking at a computer task: 11.a illustrates the distributions for the whole range; 11.b - d illustrate distributions for luminance ranges of 0 to 1000, 500, and 100, respectively.

2.2.1.4 Evaluation by Luminance Contrast:

Luminance contrast is a metric for studying the relationship between the luminances of a target and background. A target that is larger than the minimum size is visible to the human eye only if it differs from its immediate background in luminance or color [20]. Luminance contrast can be calculated as follows:

$$C = \left| \frac{(L_t - L_b}{L_b} \right| \qquad \textit{(Equation 4)}$$

L_t = *luminance of the target*
L_b = *Luminance of the background*

Calculated contrast takes values between 0 and 1, if target is darker than the background. Veiling reflections (i.e. reflections from specular or glossy surfaces) reduce the contrast of a visual task. The threshold contrast (contrast of a target that is detected 50% of occasions) varies based on many factors such as target size, retinal illuminance, and age. Contrast threshold value of 0.02 - 0.05 can be taken as a representative value for all but smallest objects seen in typical windowless offices, which have luminance values of 50-250 cd/m^2 [26]. This value is a threshold for defining task visibility, so it is not appropriate as a design goal. Studies show that contrast above 0.4 has very small effect on visibility for black and white tasks [20, 26, 27], and therefore it can be chosen as a minimum design goal.

The task contrast for the screen and the paper are calculated based on luminance of black and white squares, where black represents the text while white represents the background. The calculated contrast values for the scene in Fig. 12 are 0.93 and 0.94 for computer and paper tasks, respectively. Note that the maximum contrast for this task is 0.995, based on the minimum and maximum luminance values produced by the screen (measured as 230 and 1.2 cd/m2 in a dark room). The contrast on a computer screen is calculated at two different times, with 3 different modes of shade operation. Fig. 14.a-f demonstrate the volume seen by the computer screen throughout the contrast measurements. Both sets of images (a-c and d-f) are taken with direct solar radiation on the façade, but the second set represents a time when the sun orb can be seen through the window, thus it can provide a potentially challenging situation in terms of veiling reflections. The contrast values are given in Table 3. In all cases, the contrast is measured well above the design goal. Since the workstation is located sufficiently further away from the façade, no direct solar radiation reaches the computer screen that causes troublesome veiling reflections.

Table 3 Luminance contrast on screen

Base	Fig. 12	Fig. 14.a	Fig. 14.b	Fig.14.c	Fig. 14.d	Fig.14.e	Fig.14.f
0.995	0.93	0.82	0.82	0.89	0.79	0.85	0.90

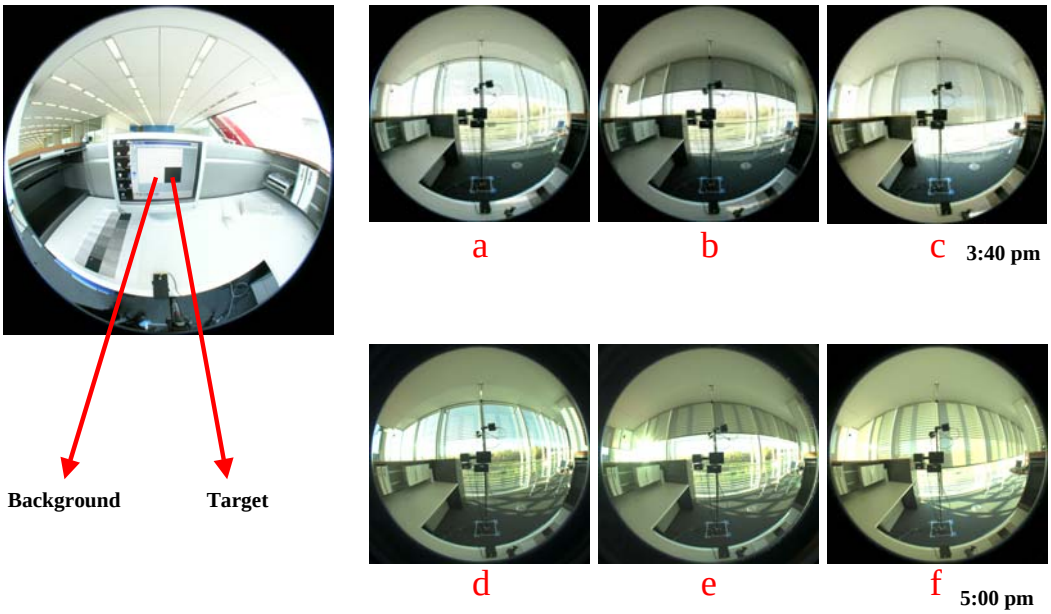

Fig. 14 Contrast on computer screen. 14a-f illustrate the volume seen by the computer screen at two different times with 3 modes of shade fabric (Multiple exposure images are taken on 10/26/2004 between a) 15:32:59 - 15:33:45 b) 15:36:09 - 15:36:53 c) 15:39:25 – 15:40:06 d) 16:51:14 - 16:52:01 e) 16:56:43 - 16:57:35 f) 16:59:24 - 17:00:24; aperture size of f/4; shutter speed between 1/15 - 1/4000 sec; clear sky)

2.2.1.4 Evaluation by Visual Field of View:

The images can also be analyzed by dissecting into various regions. Fig. 15 illustrates parts of the visual field; i.e. foveal vision, binocular vision and the peripheral vision. The human visual system can be quite insensitive to large luminance differences in the total field of view, but it is very sensitive to small luminance differences in the foveal region. This kind of analysis is helpful for understanding of the performance of the human vision and (transient) adaptation.

> **"***Foveal vision is the seeing of objects in the fovea, which is approximately the 2° in the central part of the visual field. It permits seeing much finer detail than does peripheral vision. Binocular vision is the seeing of the portion of space where the fields of the two eyes overlap. Peripheral vision is the seeing of objects displaced from the primary line of sight and outside the central visual field" [20].*

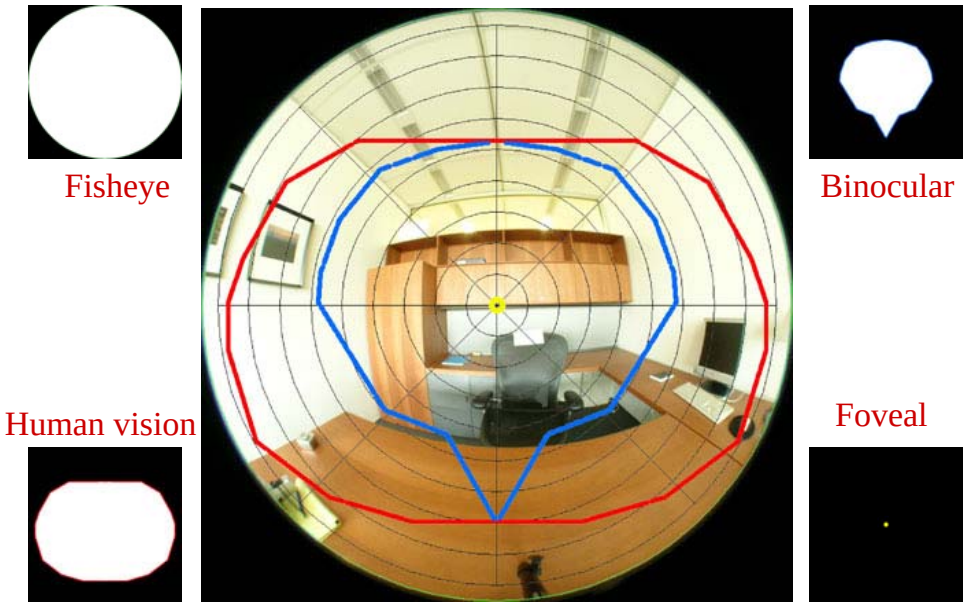

Fig.15 Demonstration of the human field of view when the user is looking towards the interior in one of the executive offices in the mockup building (Multiple exposure images are taken on 10/27/2004 between 12:59:17 – 13:00:06; aperture size of f/4; shutter speed between 1 - 1/60 sec; clear sky)

Fig. 16 demonstrates the fields of 30°, 60°, and 90° in diameter when the user is looking towards the west façade in one of the executive offices in the mockup building. The average luminance values for 30°, 60°, and 90° cones are 24.7, 17.4, and 18.5 cd/m^2. These cones can be used to check the luminance ratios between task and immediate surrounding (30°) and distant surrounding (60°), and anywhere within the field of view (90°) as 3:1, 10:1 and 40:1, respectively. The task is taken as the central 2° in the image (i.e. the occupant's eye is assumed to be fixated) in Fig. 16 and the luminance ratios are calculated as 1.4:1, 2:1, 1.9:1, respectively. The ratios are within IESNA recommendations.

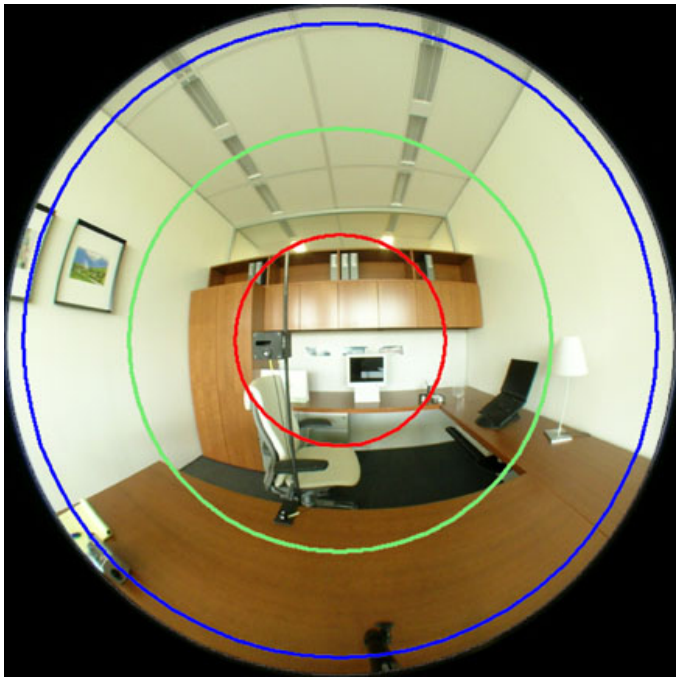

Fig.16 Demonstration of the 30°, 60°, and 90° in diameter when the user is looking towards the interior in one of the executive offices in the mockup building (Multiple exposure images are taken on 10/27/2004 between 12:51:25 – 12:52:18; aperture size of f/4; shutter speed between 1 - 1/60 sec; clear sky)

3. REMARKS

This report presents a framework for utilizing per-pixel data captured in complex settings to analyze the qualitative and quantitative aspects of lighting. The techniques are the syntheses of the current practices in lighting design and the unique practices that can be done with per-pixel data availability. They are not exhaustive in nature; rather, they highlight some of the capabilities that can be used by lighting designers, researchers, and educators.

Per-pixel data analysis provides three distinct benefits:

1. It improves the information input and accelerates the calculation process for the available analysis techniques (example: glare calculations).
2. It facilitates new analysis methods and human factor studies by providing detailed information about the luminous environment. We are collaborating with the National

Research Council of Canada on utilizing per-pixel measurement and analysis techniques in human factor studies.

3. It creates a flexible analysis medium, where analysis methods can be customized based on the needs of the design or research project. For example, an analysis that is not discussed in this report incorporates the utilization of the per-pixel data measurement/analysis technique to document the photometric properties of light sources in terms of luminance distribution patterns. This approach is easier to measure and more intuitive than analyzing the candle power distribution of light sources. This technique is being utilized at LBNL to measure and analyze the distribution of LED light sources. Another innovative example is to use per-pixel data to measure the angular reflectance and transmittance properties of materials.

The current implementation of the per-pixel analysis techniques is not provided through a Graphic User Interface (GUI). A flexible and comprehensive GUI is suggested for wide-ranging usage.

ACKNOWLEDGEMENTS:

This work was supported by the Assistant Secretary for Energy Efficiency and Renewable Energy, Office of Building Technology, Building Technologies Program, of the U.S. Department of Energy under Contract No. DE-AC02-05CH11231. I thank Glenn Hughes from New York Times for providing access to the New York Times Headquarters mockup building, where I have taken the pictures used in this report.

REFERENCES

[1] Miller N. Task Ambient Office Lighting Technology, Trends, and Research. Report prepared for the Lawrence Berkeley National Laboratory, Lighting Research Group, May 2003.

[2] Inanici MN and Galvin J. Evaluation of High Dynamic Range Photography as a Luminance Mapping Technique. Lawrence Berkeley National Laboratory, Lighting Research Group, LBNL-Report # 57545, Berkeley, CA, December 2004.

[3] Lawrence Berkeley National Laboratory. Radiance Lighting Simulation and Rendering System. <http://radsite.lbl.gov>.

[4] Mitsunaga, T. and Nayar, S.K. "Radiometric Self Calibration", Proceedings of IEEE Conference on Computer Vision and Pattern Recognition, Fort Collins, June, 1999.

[5] Debevec, P.E. and Malik, J. "Recovering High Dynamic Range Radiance Maps from Photographs", ACM SIGGRAPH Proceedings of the 24th Annual Conference on Computer Graphics and Interactive Techniques, 1997, 369-378.

[6] Inanici MN. Transformations in Architectural Lighting Analysis: Virtual Lighting Laboratory [dissertation]. Ann Arbor, MI: University of Michigan, 2004. Available from: ProQuest Information and Learning, Ann Arbor, MI; AAT 3121949.

[7] Ward, G. "Real pixels". In Graphics Gems II, (Arvo, J. (ed)). Boston: Academic Press, Inc., 1991.

[8] Lawrence Berkeley National Laboratory. Radiance Programs: Glare, http://radsite.lbl.gov/radiance/man_html/glare_1.htm

[9] Ward, G. Photosphere, http://www.anyhere.com/.

[10] Lawrence Berkeley National Laboratory. Radiance Programs: Falsecolor, http://radsite.lbl.gov/radiance/man_html/falsecolor.1.html.

[11] Lawrence Berkeley National Laboratory. Radiance Programs: Findglare, http://radsite.lbl.gov/radiance/man_html/findglare.1.html.

[12] Lawrence Berkeley National Laboratory. Radiance Programs: Glarendx, http://radsite.lbl.gov/radiance/man_html/glarendx.1.html

[13] Lawrence Berkeley National Laboratory. Radiance Programs: Xglaresrc, http://radsite.lbl.gov/radiance/man_html/xglaresrc.1.html

[14] Wienold, J, Reetz C, and Kuhn T. “Evalglare”, Fraunhofer Institute for Solar Energy Systems, Germany, http://www.ise.fraunhofer.de/radiance

[15] Ward, G. “RADIANCE Visual Comfort Calculation”, 1992, http://radsite.lbl.gov/radiance/refer/Notes/glare.html.

[16] Chauvel, P., Collins, J.B., Dogniaux, R., and Longmore, J. “Glare from Windows: Current Views of the Problem”. Lighting research and Technology, v. 14, no 1, 1982, pp. 31-46.

[17] Hopkinson, R.G., Bradley, and Hopkinson. “A Study of Glare from Very Large Sources”. (1962). Reprinted in Architectural Physics: Lighting. Hopkinson, R.G. London: Her Majesty’s Stationary Office, 1963.

[18] Hopkinson, RG. “Glare from Daylighting in Buildings”. Applied Ergonomics, v. 3, no 4, 1972, pp. 206-215

[19] Boubekri, M. and Loyer, L.L. “Effect of Window Size and Sunlight Presence on Glare”. Lighting Research and Technology, v. 24, no 2, 1992, pp. 69-74.

[20] Rea, M.S. ed. *The IES Handbook*. 9. Ed., 1999.

[21] Luckiesh, M. and Guth, S.K. “Brightness in Visual Field at Borderline between Comfort and Discomfort (BCD)” (1949). Reprinted in Selected Papers on Architectural Lighting. Rea, M.S. ed. Washington: SPIE Optical Engineering Press, 1992, pp. 155-175.

[22] Advanced Lighting Guidelines, New Buildings Inc., 2001.

[23] Matlab, Image Processing Toolbox for Use with MATLAB, User’s Guide, Version 2, 1997.

[24] PhotoShop, http://www.adobe.com/products/photoshop/main.html

[25] Lawrence Berkeley National Laboratory, Procurement Specifications, Daylighting the New York Times Headquarters Building, http://windows.lbl.gov/comm_perf/pdf/NYT_RShades-Spec12-31-04.pdf

[26] Rea, M. “Solving the Problem of VDT reflections”, Progressive Architecture, Oct. 1991, 35-40.

[27] Boyce, P. Human Factors in Lighting. London: Taylor and Francis, 2003.